Retinal histogenesis in an altricial avian species, the zebra finch (*Taeniopygia guttata,* Vieillot 1817)

Guadalupe Álvarez-Hernán,[1,*] Elena Sánchez-Resino,[1,*] Ismael Hernández-Núñez,[1] Alfonso Marzal,[2] Joaquín Rodríguez-León,[3] Gervasio Martín-Partido[1] and Javier Francisco-Morcillo[1] (iD)

[1]*Área de Biología Celular, Departamento de Anatomía, Biología Celular y Zoología, Facultad de Ciencias, Universidad de Extremadura, Badajoz, Spain*
[2]*Área de Zoología, Departamento de Anatomía, Biología Celular y Zoología, Facultad de Ciencias, Universidad de Extremadura, Badajoz, Spain*
[3]*Área de Anatomía Humana, Departamento de Anatomía, Biología Celular y Zoología, Facultad de Medicina, Universidad de Extremadura, Badajoz, Spain*

Abstract

Comparative developmental studies have shown that the retina of altricial fish and mammals is incompletely developed at birth, and that, during the first days of life, maturation proceeds rapidly. In contrast, precocial fish and mammals are born with fully differentiated retinas. Concerning birds, knowledge about retinal development is generally restricted to a single order of precocial birds, Galliformes, due to the fact that both the chicken and the Japanese quail are considered model systems. However, comparison of embryonic pre-hatchling retinal development between altricial and precocial birds has been poorly explored. The purpose of this study was to examine the morphogenesis and histogenesis of the retina in the altricial zebra finch (*Taeniopygia guttata*, Vieillot 1817) and compare the results with those from previous studies in the precocial chicken. Several maturational features (morphogenesis of the optic vesicle and optic cup, appearance of the first differentiated neurons, the period in which the non-apical cell divisions are observable, and the emergence of the plexiform layers) were found to occur at later stages in the zebra finch than in the chicken. At hatching, the retina of *T. guttata* showed the typical cytoarchitecture of the mature tissue, although features of immaturity were still observable, such as a ganglion cell layer containing many thick cells, very thin plexiform layers, and poorly developed photoreceptors. Moreover, abundant mitotic activity was detected in the entire retina, even in the regions where the layering was complete. The circumferential marginal zone was very prominent and showed abundant mitotic activity. The partially undifferentiated stage of maturation at hatching makes the *T. guttata* retina an appropriate model with which to study avian postnatal retinal neurogenesis.

Key words: altricial; birds; development; histogenesis; morphogenesis; precocial; retina.

Introduction

Birds show a wide range of variation in functional maturity at hatching and dependence on parental care. In accordance with these differences, birds are separated into precocial and altricial species. The incubation period is longer in precocial birds than in altricial ones. Precocial hatchlings are covered with feathers, have open eyes, a well-developed muscular-skeletal system, and are able to feed on their own. Altricial birds, on the other hand, are born naked, blind, with less developed locomotion organs, and are completely dependent on their parents for feeding (Nice, 1962; Stark & Ricklefs, 1998).

In comparative embryological studies of birds, although the ontogenetic sequence events remained the same, the onset and offset times show variations and present different durations between altricial and precocial development (Köppl et al. 2005; Olea & Sandoval, 2012; Murray et al. 2013; de Almeida et al. 2015; Olea et al. 2016). As a general rule, those works have shown that precocial species reach the early stages of development in less time than altricial species. In the latter stages, these differences become striking, as the last stages of precocial species are characterized

by growth (Hamburger & Hamilton, 1951), whereas in altricial species, still-maturing structures are present (Murray et al. 2013). Therefore, the last stages of development prior to hatching may explain the increased maturation of tissues observable in precocial species at hatching day compared with altricial species.

Important differences in the degree of maturation have also been found at birth in the retina of other classes of vertebrates. Thus, altricial fish species have shorter incubation times and hatch with a relatively simple retina and do not complete retinal development until late in larval life (Bejarano-Escobar et al. 2009, 2010, 2014, 2015; Pavón-Muñoz et al. 2016). In contrast, precocial fish species, with a major embryological development, complete retinal maturation before hatching (Candal et al. 2005, 2008; Harahush et al. 2009; Ferreiro-Galve et al. 2010; Bejarano-Escobar et al. 2012, 2013, 2014, 2015). In most species of mammals, including the mouse and the rat, the retina is incompletely developed at birth, and maturation proceeds rapidly during the first weeks of life (Young, 1985ab; Rapaport et al. 2004; Bejarano-Escobar et al. 2011). In the guinea pig, pig, and human, the retina is well developed at birth (Loeliger & Rees, 2005; Hendrickson et al. 2007; Nag & Wadhwa, 2007; Guduric-Fuchs et al. 2009). Data concerning ontogeny of the visual system in precocial bird species such as the chicken (*Gallus gallus* Linnaeus 1758) (Prada et al. 1991; Bruhn & Cepko, 1996; Francisco-Morcillo et al. 2005; Bejarano-Escobar et al. 2015) and Japanese quail (*Coturnix japonica*, Temminck and Schlegel 1849) (Marín-Teva et al. 1999a,b,c; Kubota et al. 2002) are also abundant. These species hatch with a completely mature retina. However, it has been described that endogenous stem cells located in the peripheral-most region of the retina, called the circumferential marginal zone (CMZ), add new neurons to the retinal tissue during the first postnatal weeks (Fischer & Reh, 2000; Kubota et al. 2002).

Despite their importance, reports covering embryonic visual system development in altricial birds are rare, probably owing to the difficulty in accessing embryonic specimens due to the dependence on parental care and the low reproduction rates of altricial forms. The zebra finch (*Taeniopygia guttata*, Vieillot 1817) is well known for its vocal learning abilities. These abilities depend on progenitor cells located in the ventricular zone of the telencephalon that give rise to song-control neurons that contribute to the construction of brain areas important for song-learning (Dewulf & Bottjer, 2005; Charvet & Striedter, 2008, 2011). Therefore, *T. guttata* is considered an excellent model with which to study postnatal neurogenesis in the central nervous system. However, very little is known about the visual system neurogenesis of this altricial species. We used classical histological and immunohistochemical methods: (i) to carry out a detailed chronological description of the most relevant morphogenetic and histogenetic events during retinal development in *T. guttata*; (ii) to determine the degree of maturation of the retina in hatchlings; (iii) to compare our results with those described in *G. gallus* in order to identify possible differences in development between precocial and altricial bird species.

Material and methods

Animals and tissue processing

All animals were treated according to the regulations and laws of the European Union (EU Directive 2010/63/EU) and Spain (Royal Decree 53/2013). A total of unrelated 12 zebra finch pairs were obtained from a local pet shop and distributed in two indoor aviaries (1 × 3 × 2 m). The aviaries were made of plywood with mesh wire roofs and front panels, thus allowing acoustic but not visual contact between animals in adjacent aviaries. Aviaries had air temperatures of 19–35 °C. Birds were kept in *ad libitum* feeding conditions throughout the experiment. They were supplied daily with Senegal, plata, and red millet seeds both dried and germinated, and fresh water (with vitamins added three times a week). Each aviary was equipped with 12 wooden nest-boxes (12.5 × 12 × 14 cm) and with coconut fibre as nesting material put on the floor before the birds were introduced.

Captive zebra finches usually lay one egg per day. All eggs were collected approximately 5 h after lights came on in the morning. Upon collection, eggs were placed within a rotating egg incubator designed for chicken eggs (Masallés S.A.). The incubator was maintained at 37.5 ± 1 °C and 80–90% humidity. The eggs were placed in a small padded dish on the rotating bars of the incubator. They roll within the dish, preventing embryo adhesion to the shell interior. At this temperature the average time of incubation was 14 days, similar to the length of time required for a zebra finch egg to hatch under natural incubation. A total of 31 embryos and one hatchling were included in the present study (Table 1). The degree of development of the *T. guttata* embryos was estimated according to the stages (St) established by Murray et al. (2013). These stages are based on external anatomical features, and numbered from 1 (pre-streak stage) to 46 (postnatal day 0, P0, newly hatched chick). The embryos included in the present study ranged from St11 to St45 (Table 1). Figure 1 shows embryos belonging to several

Table 1 Staging according to Murray et al. (2013) of the *Taeniopygia guttata* embryos included in the present study.

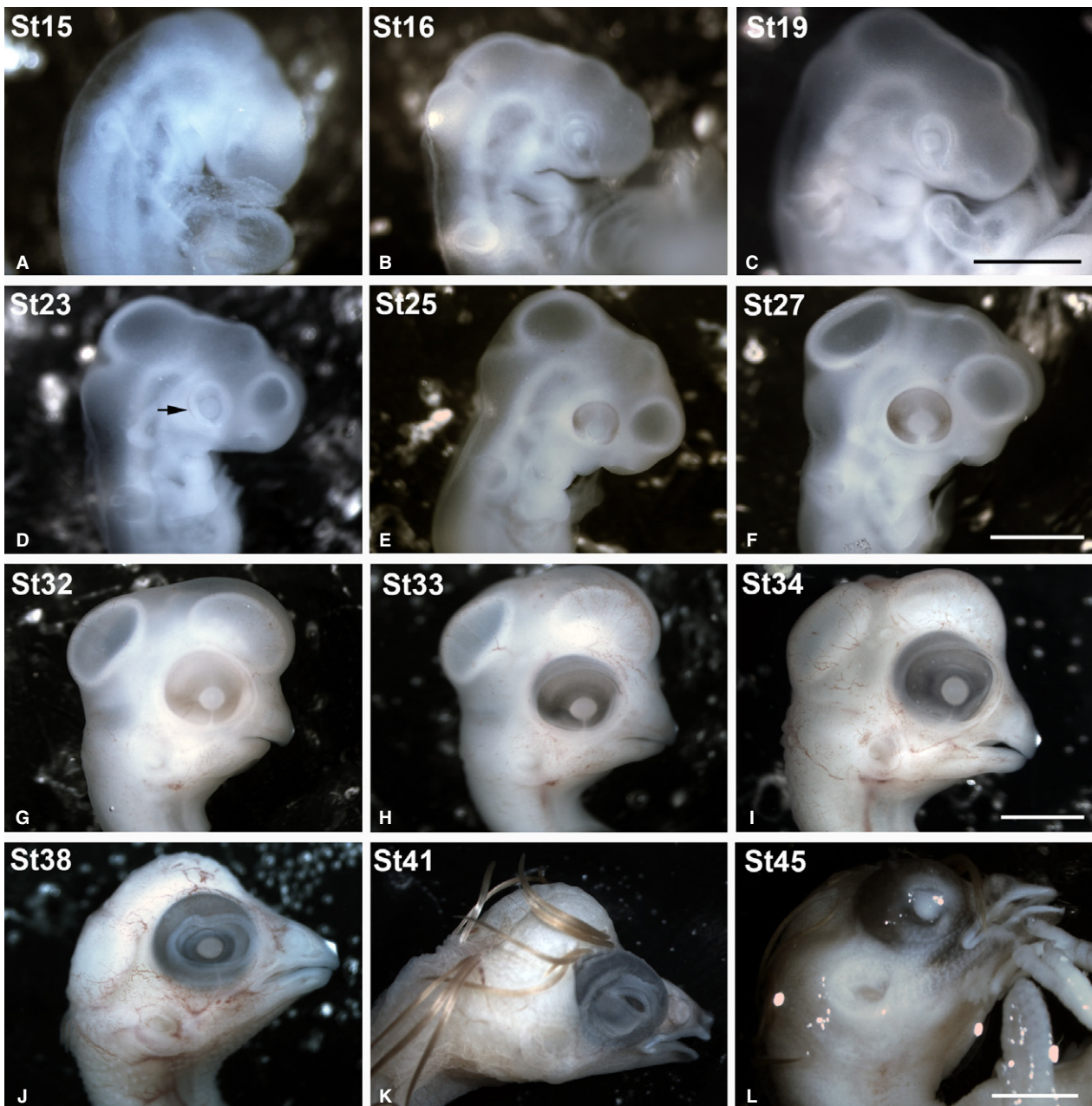| Stages	*n*	Incubation time (approximate)
St11	2	54 h
St15	2	66 h
St16	2	72 h
St19	2	84 h
St23	2	104 h
St25	2	114 h
St27	2	126 h
St32	3	6 days and 18 h
St33	3	7 days
St34	3	7 days and 6 h
St38	3	8 days and 12 h
St41	3	10 days
St45	2	13 days
St46 (postnatal day 0, P0)	1	14 days

Fig. 1 *Stereomicroscope images of some of the embryos included in the present study showing the external gross anatomical changes of the eye. The Taeniopygia guttata embryos were staged according developmental stages (St) established by Murray et al. (2013). The optic cup was clearly distinguishable between St15 and St23 (A–D). A faint pigmentation in the RPE was first observed at St23 in the caudal region of the optic cup (arrow in D). At St27, the eye was completely pigmented (F). From St38 until perinatal stages, the eyelids progressively covered the eye (J,K,L). RPE, retinal pigment epithelium. Scale bars: 2 mm (A–D); 4 mm (E,F); 6 mm (G); 7 mm (H); 10 mm (I–K).*

developmental stages. All embryos were fixed with paraformalde-hyde (PFA) 4% in phosphate-buffered solution (PBS) (0.1 M, pH 7.4) overnight at 4 °C. For morphological analysis, some fixed embryos were dehydrated in a graded series of acetone and propylene oxide, and embedded in Spurr's resin. Serial frontal 3-μm sections were cut in a Reicher Jung microtome. For immunohistochemical analysis, tissues were rinsed in PBS, then cryoprotected, soaked in embedding medium and frozen. Cryostat sections, 18 μm thick,

were thaw-mounted on SuperFrost Plus slides, air-dried and stored at −80 °C.

Toluidine-blue staining

Morphological analysis of development of the visual system was done on resin sections, stained with a toluidine blue 0.5% and sodium tetraborate 0.5% solution. To do the staining, the slides

were put with the colourant at 90 °C for 45 s and then rinsed with water. Slides were mounted with Eukitt® (Orsa Tec).

Immunohistochemistry

Cryostat sections were washed several times in 0.1% Triton-X-100 in PBS (PBS-T) and then pre-blocked in 0.2% gelatin, 0.25% Triton X-100, Lys 0.1 M in PBS (PBS-G-T-L) for 1 h. Sections were incubated overnight with mouse anti-SV2 monoclonal antibody (1 : 100; Developmental Studies Hybridoma Bank), mouse anti-PCNA monoclonal antibody (1 : 200; Abcam, PC10, Ab29) or rabbit anti-phospho-Histone H3 (pHisH3) polyclonal antibody (1 : 500; Millipore, Ref. 06-570) in a humidified chamber at room temperature (RT). On the second day, slides were washed twice in PBS-T and once more in PBS-G-T, and then incubated in Alexa Fluor 594 goat anti-mouse IgG (1 : 200; Molecular Probes, the Netherlands; Ref. A11032) or Alexa Fluor 488 goat anti-rabbit IgG secondary antibody solution (1 : 200; Molecular Probes; Ref. A11008), respectively, for 2 h. Sections were then washed twice in PBS-T and incubated with DAPI (4′,6-diamidino-2-phenylindole) for 10 min at room temperature. Next, the slides were washed in PBS and mounted with Mowiol (polyvinyl alcohol 40-88, Fluka, Ref. 81386).

Image acquisition and processing

Digital images of the *T. guttata* specimens were captured with a DS-5Mc (Nikon) digital camera attached to an SMZ-1000 (Nikon) stereoscopic microscope. Toluidine-blue stained sections and immunofluorescence were observed with a bright field and epifluorescence Nikon Eclipse 80i microscope, and photographed using an ultra-high-definition Nikon DXM1200F digital camera. Graphical enhancement was performed in Adobe Photoshop CS4.

Results

Retinal histogenesis was examined carefully from St11 to St46 (P0) using the toluidine-blue-stained semi-thin sections. We also labelled the cryosections immunohistochemically with antibodies against the proliferating cell nuclear antigen (PCNA), an endogenous marker for cells in the S-phase that has been used to identify precursor cells in developing and mature vertebrate retina (Candal et al. 2005; Villar-Cheda et al. 2008; Bejarano-Escobar et al. 2009, 2010). Antibodies against phosphohistone H3 (pHisH3) were also used to detect cells in the M-phase, as has been used in other studies of retinogenesis in different classes of vertebrates (Ferreiro-Galve et al. 2010; Bejarano-Escobar et al. 2012, 2014; Pavón-Muñoz et al. 2016). Additionally, to detect the onset of the emergence of plexiform layers, we used antibodies against the transmembrane synaptic vesicle glycoprotein SV2. This has been used previously to address the onset of synaptogenesis in different regions of the central nervous system of other classes of vertebrates (Bergmann et al. 1999; Blanchart et al. 2008) and also in the developing retina of fish (Bejarano-Escobar et al. 2010, 2012, 2014; Pavón-Muñoz et al. 2016), amphibians (Álvarez-Hernán et al. 2013), chick (Bergmann et al. 1999), and mammals (Okada et al. 1994). We did not find changes in the

ontogenetic features analyzed between embryos at the same embryological stage.

Retinal cytoarchitecture in *T. guttata* hatchlings

Hatchlings showed abundant ganglion cell axons in the optic nerve head (Fig. 2A) and optic nerve (Fig. 2B). The central region of the *T. guttata* retina showed the typical multi-layered structure (Fig. 2A,C). However, features of immaturity, such as ganglion cell layers (GCL) two to three cells deep, and poorly developed plexiform layers (Fig. 2A, C) were clearly distinguishable in this region. Furthermore, the somata of developing photoreceptors were arranged in two to three rows in the outer nuclear layer (ONL); outer segments were absent at this stage (Fig. 2C,E). In contrast, a neuroblastic layer (NbL) was present in the peripheral region. Immunohistochemical analysis showed abundant PCNA-immunoreactivity in the external half of the neural retina in the central and mid-peripheral regions (Fig. 3A–F). Abundant immunoreactive nuclei were also detected in the peripheral-most retina (Fig. 3A–C,G–I). Furthermore, abundant pHisH3-immunoreactive cells were detected in the ventricular surface in both the central (Fig. 4A–C,D–F) and the peripheral retina (Fig. 4A–C,G–I). Some non-apical mitoses were also distinguished in the dorso-peripheral retina (Fig. 4A–C). The strong SV2-immunoreactivity detected in both the outer plexiform layer (OPL) and the inner plexiform layer (IPL) revealed numerous synapses in the central region of the retina (Fig. 4J–L). In sum, therefore, several features of immaturity were found in the retina of hatchlings, although functional synapses were present in the plexiform layers.

Retinal development in *T. guttata*

Murray et al. (2013) have shown that optic vesicles are clearly distinguishable between St9 and St13. Histological sections of the St11 prosencephalon showed that optic vesicles expand laterally until they make contact head ectoderm (Fig. 5A,B). These paired diverticula were composed of neuroepithelial cells (Fig. 5B). At St15, the optic cup was formed and the lens placode was clearly observable (Fig. 5C,D). Mitotic figures were present in the ventricular region of the presumptive neural retina (apical mitotic divisions) (Fig. 5D). Optic cup invagination progressed between St16 and St19 (Fig. 5E–H). The lens vesicle was fully developed at St16 (Fig. 5F) and was almost entirely independent of the cephalic ectoderm at St19 (Fig. 5H). By these stages, intense mitotic activity was observed in the ventricular surface of the presumptive neural retina, and abundant extracellular spaces appeared in the vitreal region (Fig. 5F,H). The lumen of the neural tube was still connected with the lumen of the optic cup (Fig. 5E,G).

Eye morphogenesis progressed between St23 and St27. By these stages the neural retina still showed an
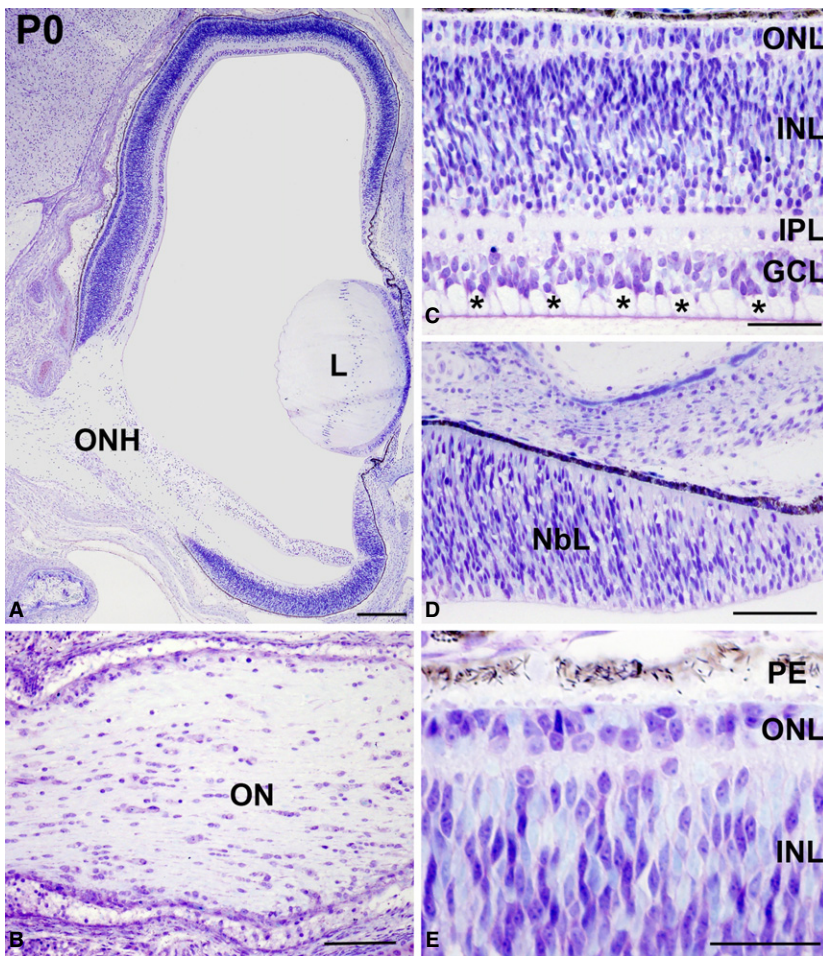
Fig. 2 Toluidine blue-stained semi-thin sections showing the retinal cytoarchitecture of *Taeniopygia guttata* hatchlings. The optic nerve head was prominent (A) and abundant ganglion cell axons were observed in the OFL (asterisks in C) and in the optic nerve (B). The layering was complete in the central retina (C). Photoreceptors were devoid of outer segments in the central retina (C,E). The peripheral retina was composed of an NbL (D). GCL, ganglion cell layer; INL, inner nuclear layer; IPL, inner plexiform layer; NbL, neuroblastic layer; OFL, optic fibre layer; ON, optic nerve; ONH, optic nerve head; ONL, outer nuclear layer; OPL, outer plexiform layer; PE, pigment epithelium. Scale bars: 200 μm (A); 100 μm (B–E).

undifferentiated aspect (Fig. 6). However, the first differentiating neuroblasts were morphologically distinguished in the vitreal region of the neuroblastic layer (NbL) at St25 (Fig. 6C). Furthermore, axon bundles in close contact with the vitreal surface appeared in the differentiating neural retina by this stage (Fig. 6C). Additionally, at St25 the first signs of pigmentation appeared in the pigment epithelium (Fig. 6C). At St27 the eye increased in size considerably (Fig. 6D) and the number of differentiated neuroblasts, mitotic figures located in the scleral retina, and fibre bundles near the vitreal surface increased notably (Fig. 6E). Optic axon bundles were also abundant in the ventral region of the distal optic stalk (Fig. 6F). The size of the eye increased progressively between St32 and St38 (Fig. 7A,D, G). The optic fibre layer (OFL) became progressively thicker (Fig. 7B,E,H). Abundant mitoses were observed in the scleral surface (Fig. 7B,C,E,F,H,I), but sparse non-apical mitoses, located vitreally in the undifferentiated retina, were also detected in the central region of the retina at St32 (Fig. 7B, B′) and in the central and peripheral retina at St34 (Fig. 7E, F) and St38 (Fig. 7H,I). These non-apical divisions were frequently vertically oriented (with the mitotic spindle aligned perpendicular to the vitreal surface) (Fig. 7B,B′), and the

vitreal mitoses were pHisH3-immunoreactive (Fig. 8A–C). At St38, the IPL became recognizable as a thin acellular region near the presumptive ganglion cell layer (GCL) in the central region of the retina (Fig. 8A,C,D,F). At this stage, SV2-immunoreactivity was detected in the OFL and ganglion cell somata, and became concentrated near the emerging IPL (Fig. 8E,F). The emergence of the outer plexiform layer (OPL) occurred at St39 in the central region of the developing retina (Fig. 8G,I); at this stage, the OPL showed faint immunoreactivity against SV2 antisera (Fig. 8H,I). Strong SV2-immunolabelling was also detected in the IPL, optic nerve head, optic nerve, and optic chiasm (Fig. 8H,I,K,L,N, O). The central-to-peripheral gradient of histogenesis and cell differentiation was clearly observed in the St41 retina: the central was divided in the three typical nuclear layers (Fig. 9A,B), the OPL was lost in the mid-peripheral retina (Fig. 9A,C), and the peripheral retina still showed a neuroepithelial organization (Fig. 9A,D). At St45, the retinal cytoarchitecture was very similar to that found in the P0 retina (not shown).

Our findings indicate that retinal maturational events appear progressively following a central-to-peripheral gradient. The emergence of the OPL was delayed with respect
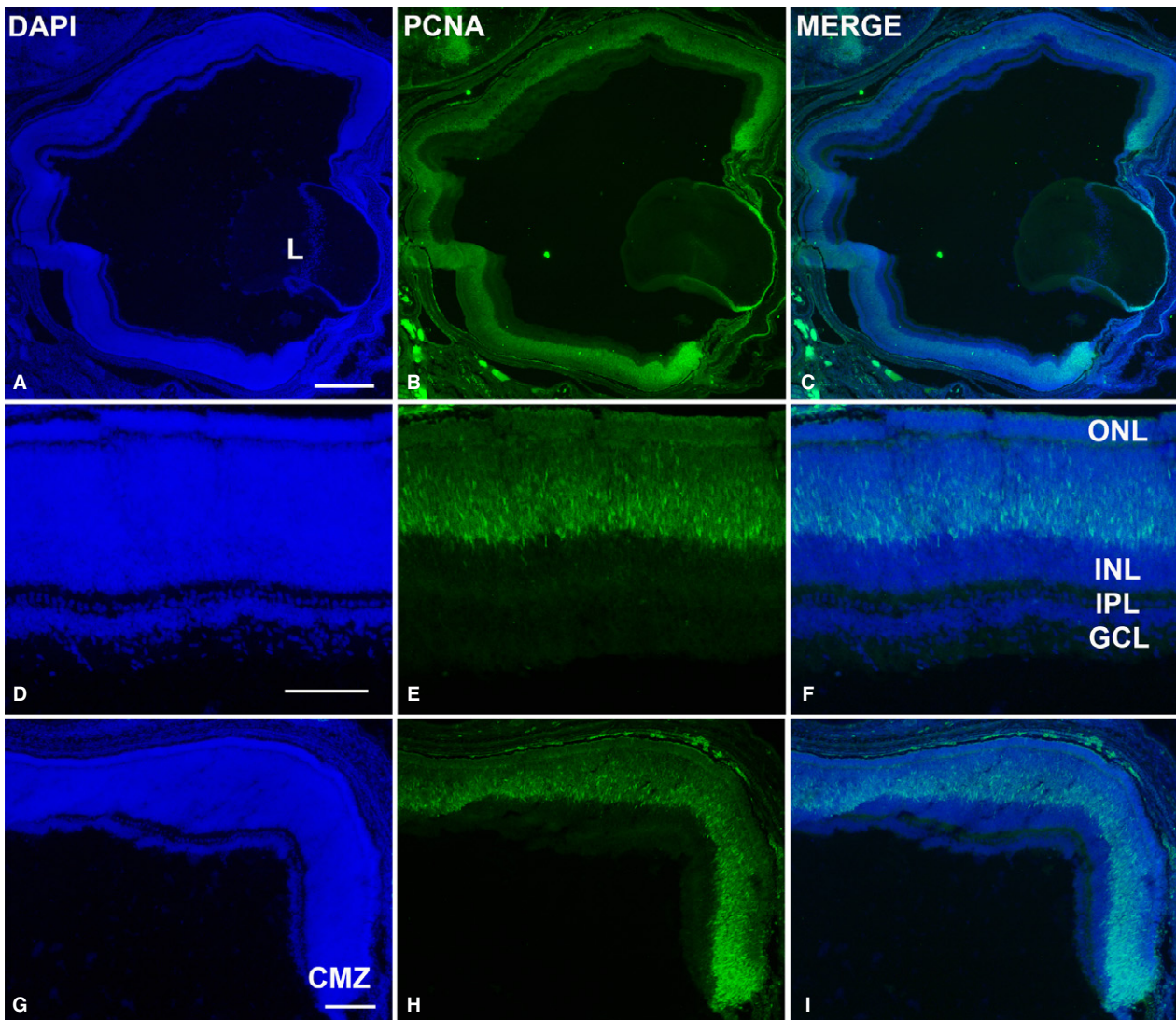
Fig. 3 PCNA-immunoreactivity in the retina of *Taeniopygia guttata* hatchlings. Abundant PCNA-positive nuclei were observed throughout the entire retina (A–C). They were restricted to the outer INL in the central retina (D–H). Proliferative activity was intense in the peripheral-most retina (G–I). GCL, ganglion cell layer; INL, inner nuclear layer; IPL, inner plexiform layer; L, lens; ONL, outer nuclear layer. Scale bars: 200 μm (A–C); 100 μm (D–I).

to the IPL, suggesting an additional vitreal-to-scleral gradient. Furthermore, the typical cytoarchitecture of the vertebrate retina was observed in almost the entire perinatal retina, but evident morphological features of immaturity were still found.

Discussion

Retinal maturity at hatching in *T. guttata*

The retina of precocial bird species such as chicken, duck or quail already has all its layers at birth and shows differentiated cells (Prada et al. 1991; Drenhaus et al. 2007; Rojas et al. 2007; Bejarano-Escobar et al. 2015). The present study

has shown that, at hatching, the layering was complete at central and mid-peripheral regions of the zebra finch retina. However, features of immaturity were still observable: ganglion cell bodies were arranged in two or three rows and the plexiform layers were poorly developed. Furthermore, photoreceptors are still undifferentiated as has been described in other altricial birds such as the pigeon *(Columba livia)* (Rojas et al. 2007) in which photoreceptor maturation extends over the first two postnatal weeks of life. Additionally, PCNA-immunoreactivity was abundant in cells located in the *T. guttata* peripheral-most retina. The number of PCNA-positive nuclei decreased progressively in cells in the INL that were located away from the retinal margin, but they were still abundant in the differentiated
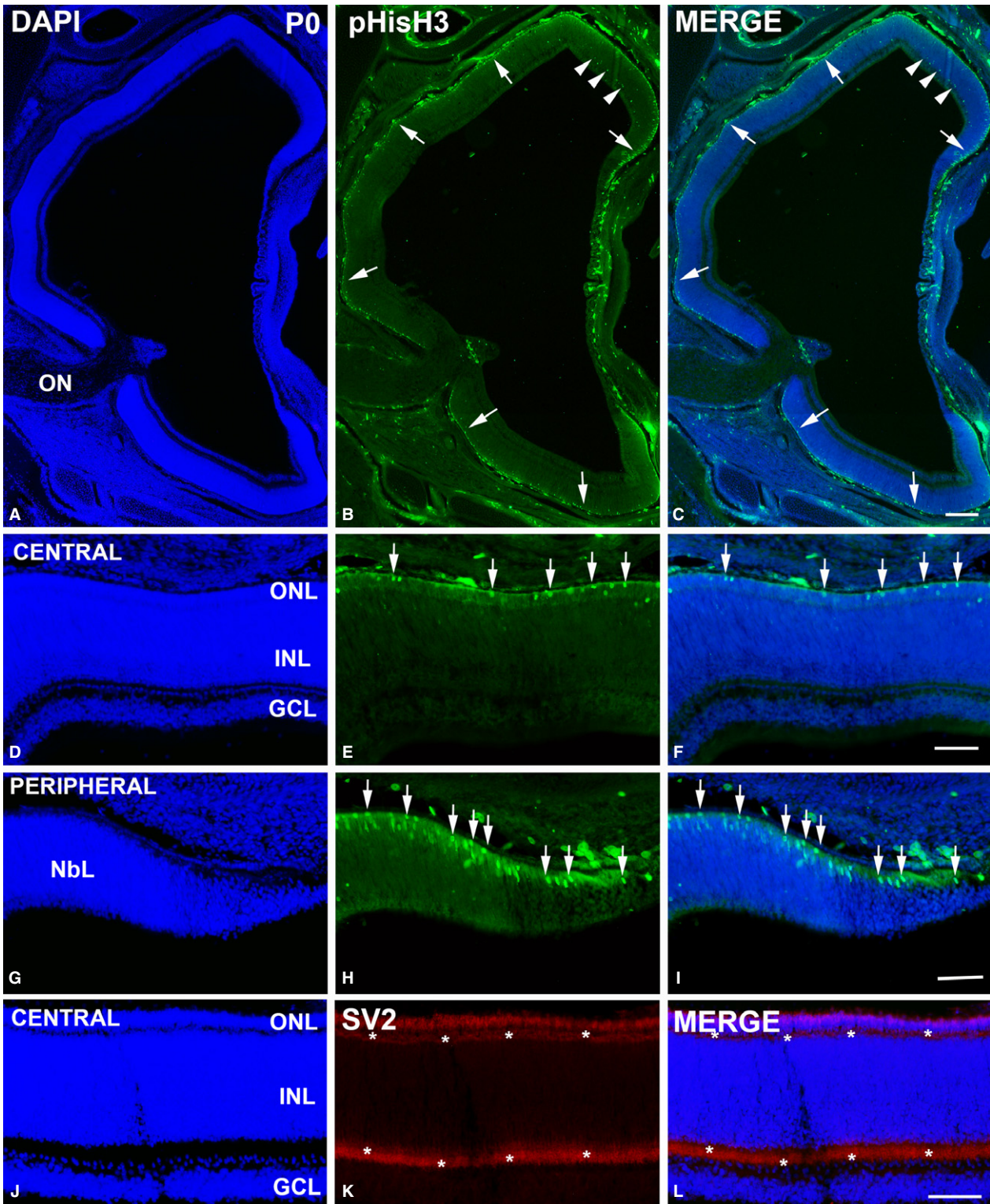
Fig. 4 pHisH3- (A–I) and SV2-immunoreactivities (J–L) in the *Taeniopygia guttata* retina at the hatching day. Apical mitoses located in the scleral surface were clearly observable in both the central and the peripheral retina (arrows in B,C,E,F,H,I). Immunoreactive non-apical mitoses were also detected in the peripheral retina (arrowheads in B,C). Plexiform layers showed no DAPI staining (A,C,D,F,J,L) but strong SV2-immunoreactivity (asterisks in K,L). GCL, ganglion cell layer; INL, inner nuclear layer; NbL, neuroblastic layer; ON, optic nerve; ONL, outer nuclear layer; OPL, outer plexiform layer. Scale bars: 200 μm (A–C); 100 μm (D–L).
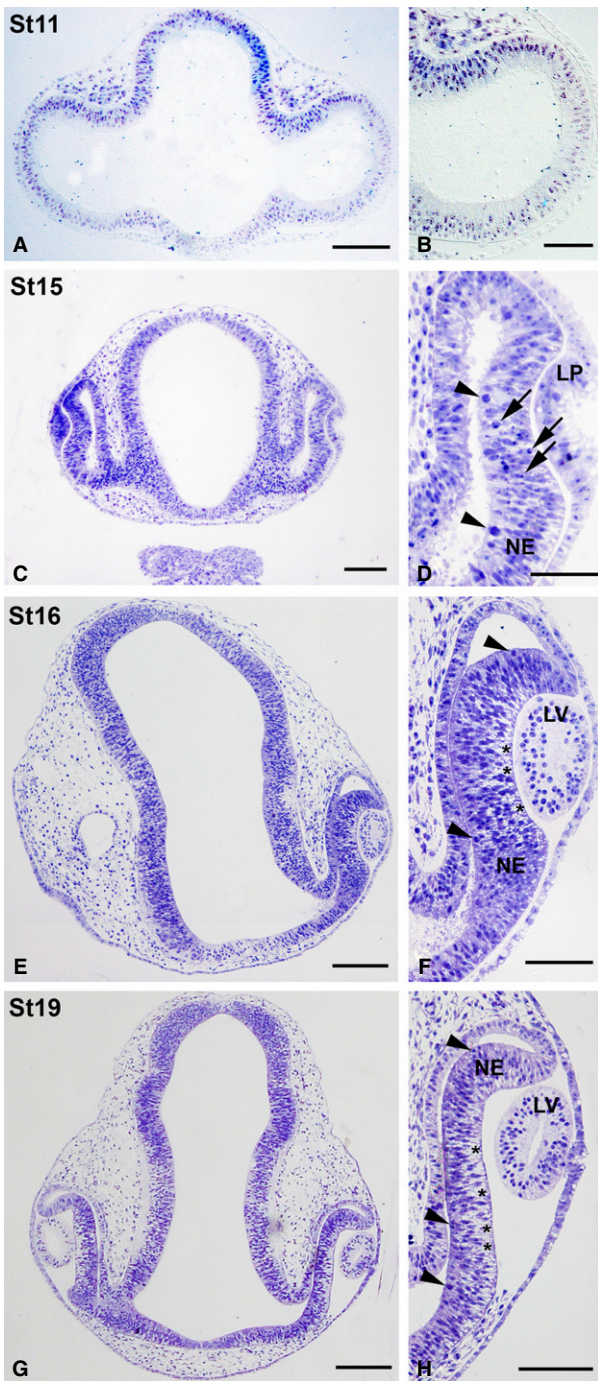
Fig. 5 Toluidine blue-stained semi-thin sections showing early stages of development of the eye rudiment in *Taeniopygia guttata*. Optic vesicles were composed of an undifferentiated neuroepithelium at St11 (A, B). Progressive invagination of the distal optic vesicle resulted in the formation of the optic cup (C–H). Many mitotic figures were seen in the scleral surface of the presumptive neural retina by these stages (arrowheads in D,F,H). The lens placode was present at St15 (C,D) and the lens vesicle could be observed by St16–St17 (E–H). Abundant pyknotic bodies (arrows in D) were observed in the presumptive neural retina at St15 (C,D) and extracellular spaces near the vitreal surface were clearly distinguishable by St16–St17 (asterisks in F,H). LP, lens placode; LV, lens vesicle; NE, neuroepithelium. Scale bars: 100 μm (A–H).

retina. PCNA-immunoreactive nuclei were mainly located in the outer INL. Abundant apical (also known as 'scleral' or 'ventricular') mitoses were observed in the laminated central and mid-peripheral *T. guttata* retina. It has been described that the cessation of cytogenesis, monitored by the disappearance of mitotic figures in the ventricular surface of the retina, is closely coincident in space and time with the development of the OPL in fish (Bejarano-Escobar et al. 2012; Pavón-Muñoz et al. 2016) and some mammals (Robinson et al. 1985; Stone et al. 1985). However, the OPL was clearly developed in *T. guttata* hatchlings and we found mitotic activity in the ventricular surface of the laminated retina. These data coincide with results obtained in the rabbit, where apical mitoses have been found in retinal regions with developed plexiform layers (Sharma & Ehinger, 1997). Abundant apical mitoses were also detected in the CMZ of hatchlings. These results showed important differences with those described for the chicken retina (Fischer & Reh, 2000). These authors have found no cells in the central retinal regions that were labelled for pHisH3, and only a few of them in the retinal margin of hatched chickens. Furthermore, the same authors also showed that PCNA was absent, except for low levels in the nuclei of photoreceptors in the central retina of postnatal chicks. They also found a small cluster of PCNA-immunolabelled nuclei at the margin of the retina. Immunoreactivity for PCNA progressively decreased in cells in the INL that were located away from the peripheral-most retina (Fischer & Reh, 2000). Therefore, the proliferative activity in the retina of *T. guttata* hatchlings is greater than that observed in hatched *G. gallus*. Moreover, the CMZ is more prominent in altricial bird species than that described for precocial birds. Therefore, in contrast to *G. gallus* where retinal neurogenesis takes place nearly exclusively during embryogenesis, abundant retinal neurons seem to be generated in *T. guttata* during post-hatch development.

Comparing these results with those found in other vertebrates, no layering was observed in the retina of altricial fish species at hatching (Evans & Browman, 2004; Bejarano-Escobar et al. 2009, 2010, 2014; Pavón-Muñoz et al. 2016). In these species, retinal histogenesis proceeded rapidly during the first 3–5 days of life. These results are in agreement with those observed in the retina of some mammals like the mouse (Sharma et al. 2003; Diao et al. 2004), albino rat (Weidman & Kuwabara, 1968), ferret (Reese et al. 1996), and gerbil (Bytyqi & Layer, 2005), where the histological evidence for the differentiation of the plexiform layers, or at least one of them, is delayed until the postnatal period. In the case of precocial species of vertebrates, the retina is fully differentiated at the time of hatching/birth in fish (Candal et al. 2005, 2008; Harahush et al. 2009; Ferreiro-Galve et al. 2010; Bejarano-Escobar et al. 2012, 2013), reptiles (Francisco-Morcillo et al. 2006), and mammals (Sharma & Ehinger, 1997; Loeliger & Rees, 2005; Nag & Wadhwa, 2007; Guduric-Fuchs et al. 2009).
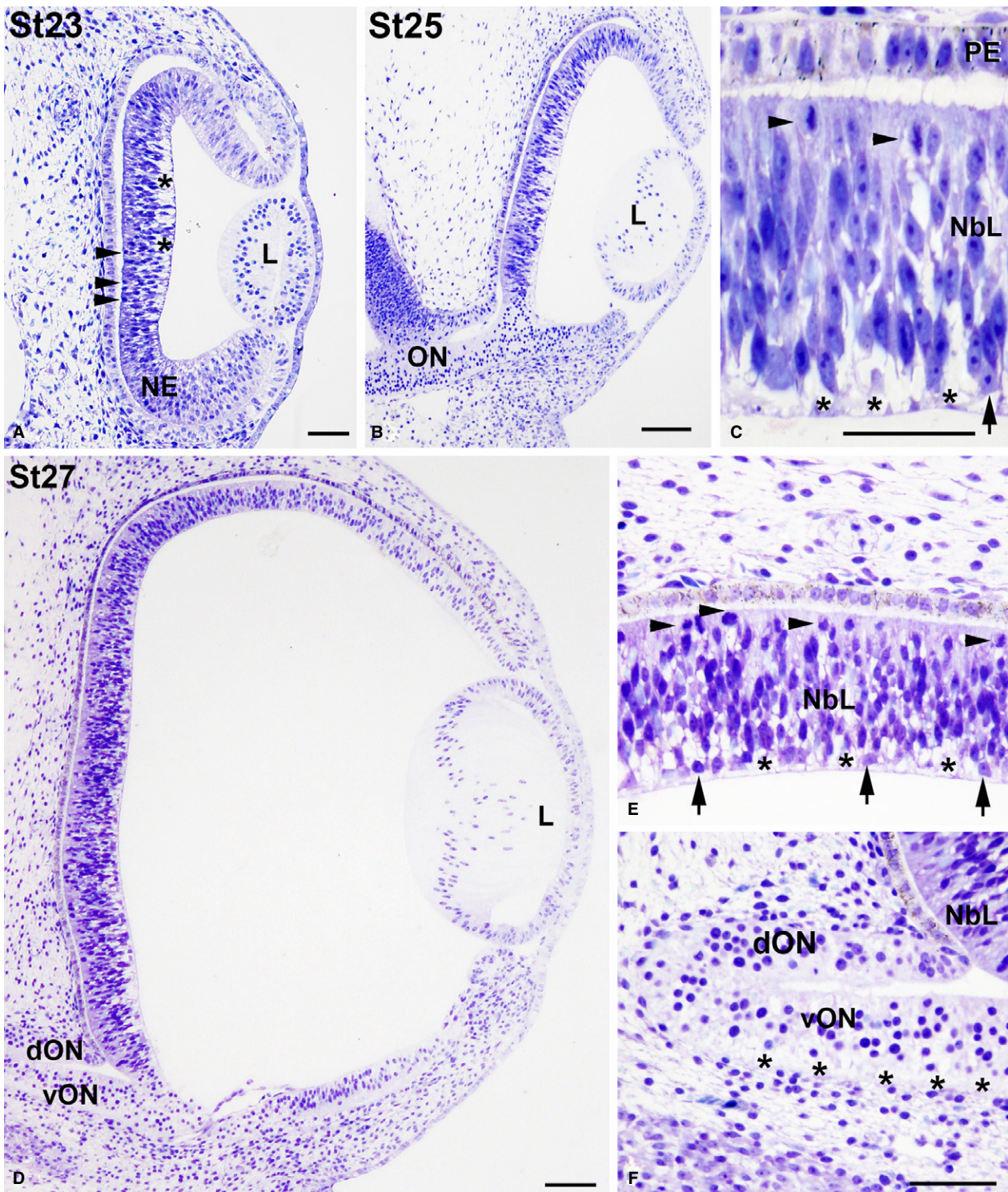
Fig. 6 Toluidine blue-stained transverse sections of the undifferentiated *Taeniopygia guttata* retina. Magnification of (B) is shown in (C), and magnifications of (D) are shown in (E,F). Lamination was absent in the developing retina between St23 and St27 (A–E). Abundant ventricular mitosis (arrowheads in A,C,E) and extracellular spaces located near the vitreal surface (asterisks in A,C,E) were observed. The neural retina is composed of NE at St23 and the first differentiated neuroblasts were observed in the vitreal region of the retina at St25 (arrow in C), increasing in number at St27 (arrows in E). Ganglion cell axons were detected in the ventral region of the ON (asterisks in F). Note that faint pigmentation was first observed in the PE at St25. dON, dorsal optic nerve; L, lens; NbL, neuroblastic layer; NE, neuroepithelium; PE, pigment epithelium; vON, ventral optic nerve. Scale bars: 100 μm (A–F).
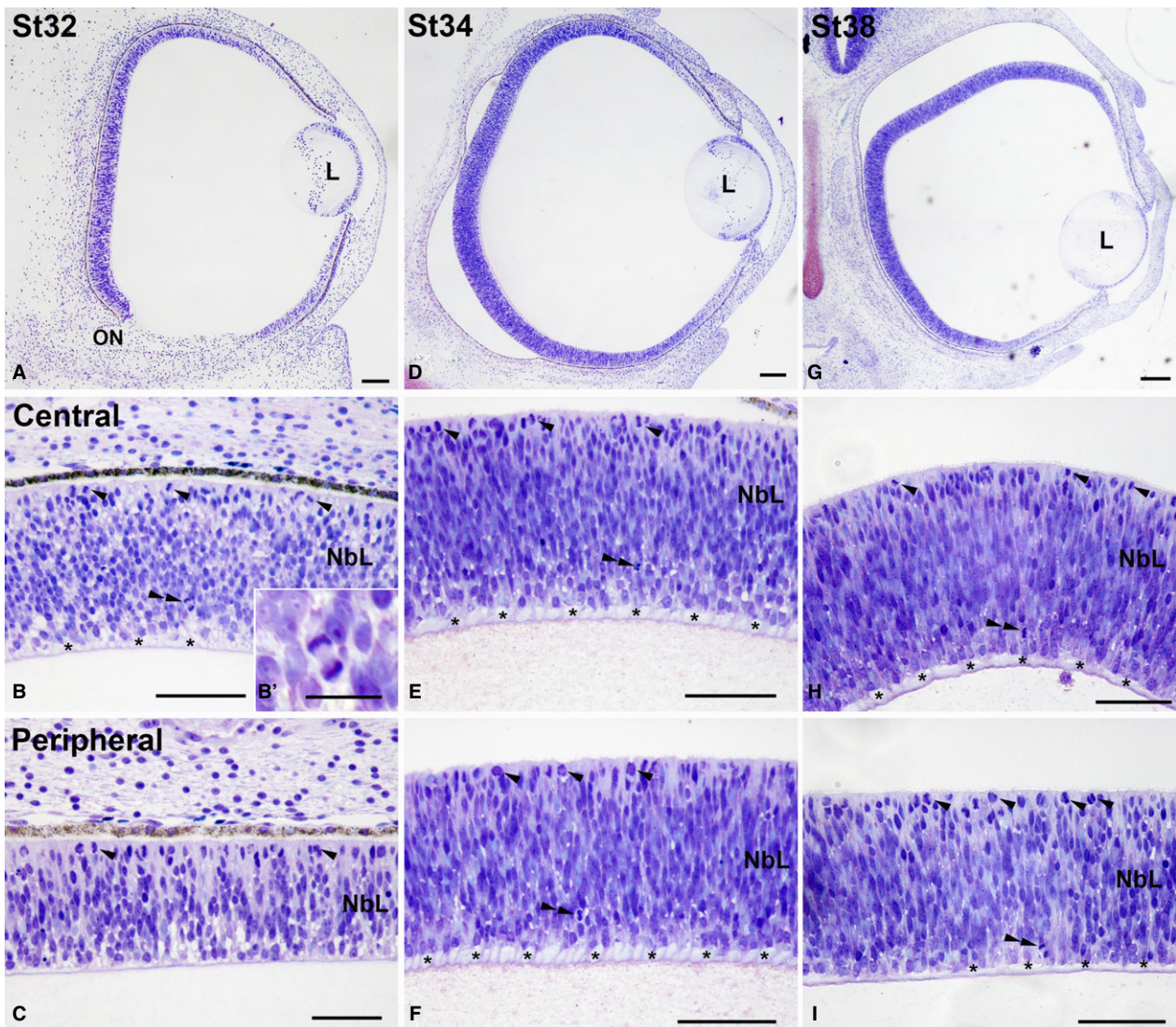
Fig. 7 Toluidine blue-stained transverse sections of *Taeniopygia guttata* developing retina. Micrographs showing the entire retina (A,D,G) and magnifications of the central (B,B',E,H) and peripheral regions (C,F,I) are shown. Abundant apical mitoses (arrowheads in B,C,E,F,H,I) and ganglion cell axons located in the vitreal surface (asterisks in B,E,F,H,I) were distinguished. Non-apical mitoses appeared in the vitreal region (double arrowheads in B,E,F,H,I). The mitotic spindle in non-apical mitoses was usually aligned perpendicular to the vitreal surface (B'). L, lens; NbL, neuroblastic layer. Scale bars: 100 μm (A–H); 30 μm (B').

Retinal morphogenesis and histogenesis in *T. guttata*

The first differentiated neuroblasts in *T. guttata* appeared in the vitreal-most region of the central retina at St24 (108 h). These early-born neurons are identified in the present paper by morphological criteria, but we have also identified them immunohistochemically with Tuj-1 antibody raised against class III β-tubulin (unpublished observations, Javier Francisco-Morcillo, JFM). The first undifferentiated neuroblasts in the chick retina have also been labelled with Tuj-1 antibody in the developing retina of the chick at stage 16 of Hamburger & Hamilton (1951) (HH16, 51–56 h, see Table 2) (Snow & Robson, 1994, 1995; Francisco-Morcillo et al. 2005).

Later in development, abundant non-apical mitoses were observed localized in the inner region of the undifferentiated *T. guttata* retina. These non-apical mitotic figures (also called 'ectopic' or 'basal' mitoses) have also been described during retinogenesis in zebrafish (Godinho et al. 2007; Weber et al. 2014), small-spotted catshark (Bejarano-Escobar et al. 2012), chick (Edqvist & Hallböök, 2004; Boije et al. 2009; Shirazi Fard et al. 2014), cat (Rapaport et al. 1985; Robinson et al. 1985), and human (Smirnov & Puchkov, 2004). Edqvist & Hallböök (2004) have shown that basal mitosis occurs in the chicken between HH24 (E4.5) and HH35 (E8-9). In the present study, non-apical mitoses were observed in the retina of *T. guttata* from St34 to St44 (E7.25–E12), later
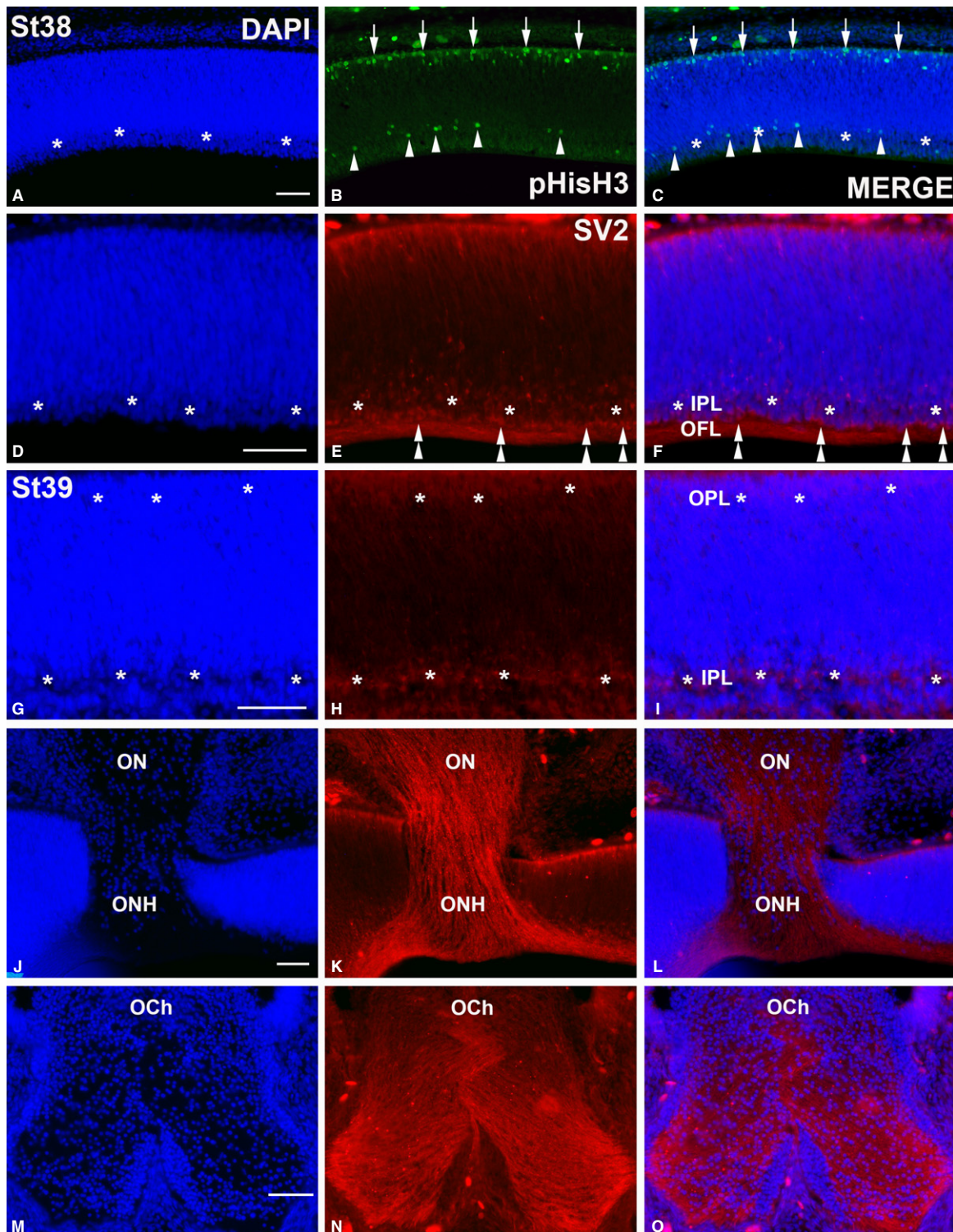
Fig. 8 pHisH3- (A–C) and SV2-immunoreactivities (D–O) in the *Taeniopygia guttata* retina and optic pathways at St38 (A–F) and St39 (G–O). Sections were counterstained with DAPI. pHisH3-immunopositive mitoses were detected in both the scleral (arrows in B,C) and vitreal regions (arrowheads in B, C). At St38, the IPL could be recognized as a DAPI-negative layer devoid of cell nuclei in the central retina (asterisks in A,C,D,F) that was faintly labelled with anti-SV2 antibody (asterisks in E,F). SV2-immunoreactivity was also detected in sparse ganglion cell perikarya (double arrowheads in E,F) and in the optic fibre layer. A poorly developed SV2-immunoreactive OPL emerged at St39 in the outer retina, whereas the IPL increased in size (asterisks in G–I). Ganglion cell axons were strongly labelled with the SV2 antisera in both the optic nerve (G–I) and optic chiasm (J–L). IPL, inner plexiform layer; OCh, optic chiasm; OFL, optic fibre layer; ON, optic nerve; ONH, optic nerve head; OPL, outer plexiform layer. Scale bars: 100 μm (A–O).

Fig. 9 Toluidine blue-stained transverse sections at St41 *Taeniopygia guttata* retina. Magnifications of the central (B), mid-peripheral (C), and peripheral (D) retina are shown. Abundant ganglion cell axons were observed in the OFL (asterisks in B,C). While retinal lamination was complete in the central retina (A,B), the OPL was absent in the mid-peripheral retina (A,C). The peripheral retina showed an undifferentiated aspect (A, D). GCL, ganglion cell layer; INL, inner nuclear layer; IPL, inner plexiform layer; L, lens; NbL, neuroblastic layer; OFL, optic fibre layer; ONL, outer nuclear layer; OPL, outer plexiform layer. Scale bars: 200 μm (A); 100 μm (B–D).
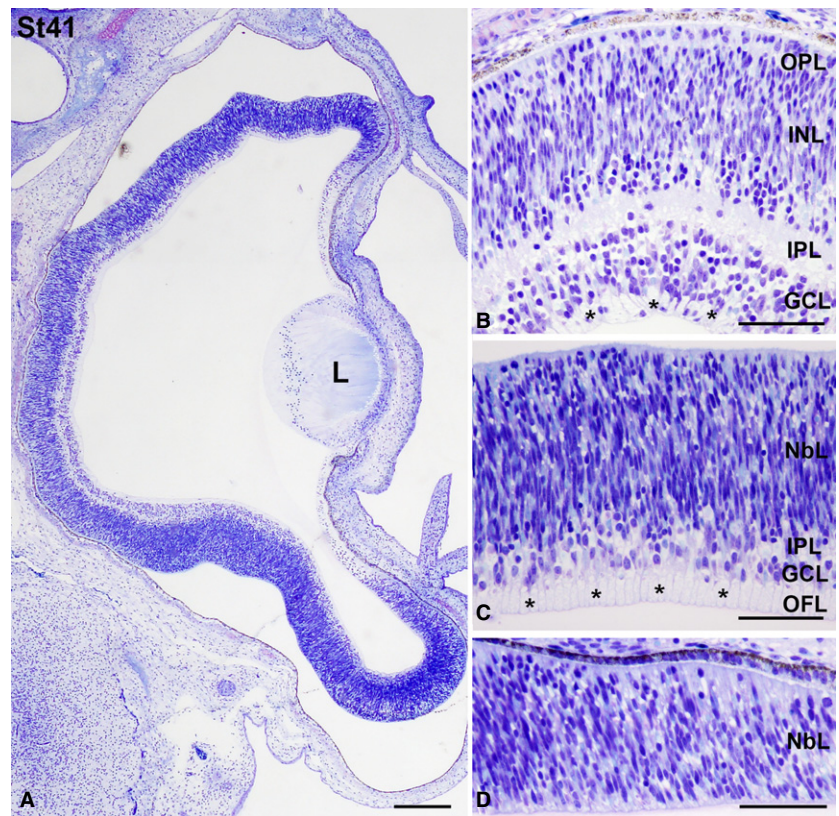
than in the chick (Table 2) (see below). During these stages, an obvious central-to-peripheral change in the pattern of appearance of mitotic figures was seen, as has been observed in the chicken (Boije et al. 2009). This coincides with the central-to-peripheral gradient of cell differentiation described for the rest of the vertebrates (Prada et al. 1991; Candal et al. 2005; Francisco-Morcillo et al. 2005, 2006; Bejarano-Escobar et al. 2009, 2010, 2012; Álvarez-Hernán et al. 2013; Pavón-Muñoz et al. 2016). Edqvist & Hallböök (2004) have also demonstrated that non-apical mitoses correspond to terminal basal mitoses undergone by horizontal cell precursors. In agreement with these results, Godinho et al. (2007) showed that these basal divisions give rise mainly to horizontal cells in the retina of teleost. However, other retinal cell types may have also been produced from these mitoses in zebrafish. Therefore, the numerous non-apical mitoses make the developing retina of *T. guttata* a pre-eminent system for studying the development of horizontal cells.

In addition to the central-to-peripheral gradient, the present paper has also shown that histogenesis progressed in a vitreal-to-scleral manner. Thus, the OPL evolved later than the IPL (Table 2), as has previously been described in the developing retina of the chick (Drenhaus et al. 2007). This delay in the OPL formation with respect to the IPL has been also detected in the retina of sharks (Harahush et al. 2009; Ferreiro-Galve et al. 2010; Bejarano-Escobar et al. 2012) and mammal species (Young, 1985a,b; Reese

et al. 1996; Rapaport et al. 2004). In contrast, the emergence of both plexiform layers occurs simultaneously in the retina of different fish species (Kitambi & Malicki, 2008; Bejarano-Escobar et al. 2009, 2010; Pavón-Muñoz et al. 2016) and turtles (Francisco-Morcillo et al. 2006). The delay of emergence between the IPL and the OPL in *T. guttata* was also monitored immunohistochemically using antibodies against SV2, which has become a powerful tool in retinogenesis studies.

Delayed visual system morphogenesis and retinal maturation in altricial species

The zebra finch is classified as an altricial bird species. The results of the present study showed that many of the morphological features that occur during visual system development, such as the formation of the optic vesicle, formation of the optic cup, early differentiation of ganglion cells, onset of appearance of non-apical mitosis, and emergence of the plexiform layers, begins earlier in *G. gallus* than in *T. guttata* (Table 2). These results are in agreement with the observations of Murray et al. (2013), which provided a detailed description of embryological development of *T. guttata* and compared developmental differences with *G. gallus.* Those workers showed that, although the total incubation time for *T. guttata* is substantially shorter than the incubation time for *G. gallus* (14 vs. 21 days, respectively), the chicken showed faster development in the early

Table 2 Chronology of different features of morphogenesis, histogenesis, and cell differentiation in the developing and hatched retina of zebra finch and chicken. St, stage (Murray et al. 2013). HH, stages of Hamburger & Hamilton (1951).

	Event	*Taeniopygia guttata*	*Gallus gallus*	References
Embryonic retina	Optic vesicle	Onset: St9 (42 h)	HH9 (29–33 h)	Murray et al. (2013) and Hamburger & Hamilton, (1951)
	Optic cup	Onset: St14 (64 h)	HH15 (50–55 h)	Hamburger & Hamilton, (1951)
	Differentiating ganglion cells	Onset: St24 (108 h)	HH16 (51–56 h)	Snow & Robson, (1994)
	Non-apical divisions	Onset: St34 (E7.25) Offset: St44 (E12)	Onset: HH24 (E4) Offset: HH35 (E8–9)	Edqvist & Hallböök, (2004) and Boije et al. (2009)
	Emergence IPL	St38 (E8.5)	HH31 (E7)	Drenhaus et al. (2007)
	Emergence OPL	St39 (E9)	HH34 (E8)	
Hatched retina	Proliferative activity	Abundant PCNA-positive nuclei both in the CMZ and outer region of the INL in the central and mid-peripheral retina	Sparse PCNA-positive nuclei in the CMZ. A few PCNA-immunopositive nuclei in the ONL of the central and mid-peripheral retina	Fischer & Reh, (2000)
		Abundant pHisH3-positive cells both in the CMZ and scleral surface of the central and mid-peripheral retina	Sparse pHisH3-positive cells restricted to the CMZ	

stages than the zebra finch did. Blom & Lilja (2005) also demonstrated that 'demand' organs such as the nervous system, muscles or skeleton develop later in altricial species compared with 'supply' organs such as the digestive organs. In contrast, precocial species exhibit slower early development of 'supply' organs and more rapid early development of 'demand' organs. Therefore, the onset and the offset of the visual system development in *T. guttata* is delayed relative to precocial bird species, such as the chicken, in both the embryonic and the postnatal period.

Conclusions and future perspectives

In young fish and amphibians, most retinal growth arises from the continuous development of new retinal tissue in a region located at the periphery of the mature tissue, the CMZ. However, the addition of new neurons from stem cell niches is diminished in postnatal birds compared with that in fish and amphibians (Amato et al. 2004; Centanin & Wittbrodt, 2014; Ail & Perron, 2017). This postnatal neurogenesis in the chicken is exclusively effected by progenitors located in the CMZ. These progenitors are restricted to producing primarily amacrine and bipolar cells (Fischer & Reh, 2000). In the present study, we have shown the existence of a prominent CMZ with abundant mitotic activity in the retina of *T. guttata* hatchlings. Furthermore, abundant mitoses were also detected in the scleral region of the laminated retina. Therefore, our findings suggest that neurogenic process in the postnatal *T. guttata* retina is intense. This partially undifferentiated stage of maturation at hatching makes the postnatal *T. guttata* retina an appropriate

model with which to study avian retinal postnatal neurogenesis. Indeed, *T. guttata* is considered to be an exceptional model with which to study adult neurogenesis in the central nervous system (for a review, see Charvet & Striedter, 2011). Thus, the major period of telencephalic neurogenesis ends approximately 1 week after hatching, although a limited amount of telencephalic neurogenesis is detected in the adult tissue (Dewulf & Bottjer, 2005; Charvet & Striedter, 2008, 2011; Striedter & Charvet, 2008). Moreover, this species also contains undifferentiated progenitor cells that contribute to an overall greater number of neurons in song-control nuclei (Dewulf & Bottjer, 2005), even during the juvenile period. The incidence and the duration of neurogenesis in post-hatched retina in *T. guttata* specimens and the factors involved in these mechanisms are subjects for future study.

Finally, the presence of stem cell niches is closely related to the regenerative capacity of the tissue. In the chicken retina, Müller glia have the potential to become progenitor cells in the avian retina (Gallina et al. 2014) and, after damage or growth-factor stimulation, an important subset of these cells can be stimulated to regenerate the adult tissue (Fischer & Reh, 2001; Fischer et al. 2014). These results make the chicken retina an excellent model for the study of regenerative processes and hence are critical to vision research in the study of human retinal pathologies. The fact that *T. guttata* is an altricial bird species allows manipulations and treatments to be performed postnatally. Our findings show that *T. guttata* is an appropriate alternative model system for the study of the mechanisms responsible for retinal regeneration.

Acknowledgements

Author contributions

G.A.H., E.S.R., and I.H.N. performed histological and immunohistochemical assays. A.M. participated in acquisition of data and critical revision of the manuscript. J.R.L., G.M.P., and J.F.M. conceived and designed the experiments and constructed figures. J.F.M. wrote the paper.

References

Ail D, Perron M (2017) Retinal degeneration and regeneration – lessons from fishes and amphibians. *Curr Pathobiol Rep* **5**, 67–78.

de Almeida HM, Sousa RP, Bezerra DO, et al. (2015) Greater rhea (*Rhea americana*) external morphology at different stages of embryonic and fetal development. *Anim Reprod Sci* **162**, 43–51.

Álvarez-Hernán G, Bejarano-Escobar R, Morona R, et al. (2013) Islet-1 immunoreactivity in the developing retina of *Xenopus laevis*. *Sci World J* **2013**, 740420.

Amato MA, Arnault E, Perron M (2004) Retinal stem cells in vertebrates: parallels and divergences. *Int J Dev Biol* **48**, 993–1001.

Bejarano-Escobar R, Blasco M, DeGrip WJ, et al. (2009) Cell differentiation in the retina of an epibenthonic teleost, the Tench (*Tinca tinca*, Linneo 1758). *Exp Eye Res* **89**, 398–415.

Bejarano-Escobar R, Blasco M, DeGrip WJ, et al. (2010) Eye development and retinal differentiation in an altricial fish species, the Senegalese sole (*Solea senegalensis*, Kaup 1858). *J Exp Zool B Mol Dev Evol* **314**, 580–605.

Bejarano-Escobar R, Holguín-Arévalo MS, Montero JA, et al. (2011) Macrophage and microglia ontogeny in the mouse visual system can be traced by the expression of Cathepsins B and D. *Dev Dyn* **240**, 1841–1855.

Bejarano-Escobar R, Blasco M, Duran AC, et al. (2012) Retinal histogenesis and cell differentiation in an elasmobranch species, the small-spotted catshark *Scyliorhinus canicula*. *J Anat* **220**, 318–335.

Bejarano-Escobar R, Blasco M, Durán AC, et al. (2013) Chronotopographical distribution patterns of cell death and of lectin-positive macrophages/microglial cells during the visual system ontogeny of the small-spotted catshark *Scyliorhinus canicula*. *J Anat* **223**, 171–184.

Bejarano-Escobar R, Blasco M, Martín-Partido G, et al. (2014) Molecular characterization of cell types in the developing, mature, and regenerating fish retina. *Rev Fish Biol Fisheries* **24**, 127–158.

Bejarano-Escobar R, Álvarez-Hernán G, Morona R, et al. (2015) Expression and function of the LIM-homeodomain transcription factor Islet-1 in the developing and mature vertebrate retina. *Exp Eye Res* **138**, 22–31.

Bergmann M, Grabs D, Rager G (1999) Developmental expression of dynamin in the chick retinotectal system. *J Histochem Cytochem* **47**, 1297–1306.

Blanchart A, Romaguera M, García-Verdugo JM, et al. (2008) Synaptogenesis in the mouse olfactory bulb during glomerulus development. *Eur J Neurosci* **27**, 2838–2846.

Blom J, Lilja C (2005) A comparative study of embryonic development of some bird species with different patterns of postnatal growth. *Zoology (Jena)* **108**, 81–95.

Boije H, Edqvist PH, Hallböök F (2009) Horizontal cell progenitors arrest in G2-phase and undergo terminal mitosis on the vitreal side of the chick retina. *Dev Biol* **330**, 105–113.

Bruhn SL, Cepko CL (1996) Development of the pattern of photoreceptors in the chick retina. *J Neurosci* **16**, 1430–1439.

Bytyqi AH, Layer PG (2005) Lamina formation in the Mongolian gerbil retina (*Meriones unguiculatus*). *Anat Embryol (Berl)* **209**, 217–225.

Candal E, Anadón R, DeGrip WJ, et al. (2005) Patterns of cell proliferation and cell death in the developing retina and optic tectum of the brown trout. *Brain Res Dev Brain Res* **154**, 101–119.

Candal E, Ferreiro-Galve S, Anadón R, et al. (2008) Morphogenesis in the retina of a slow-developing teleost: emergence of the GABAergic system in relation to cell proliferation and differentiation. *Brain Res* **1194**, 21–27.

Centanin L, Wittbrodt J (2014) Retinal neurogenesis. *Development* **141**, 241–244.

Charvet CJ, Striedter GF (2008) Spatiotemporal clustering of cell death in the avian forebrain proliferative zone. *Int J Dev Biol* **52**, 345–352.

Charvet CJ, Striedter GF (2011) Developmental modes and developmental mechanisms can channel brain evolution. *Front Neuroanat* **5**, 4.

Dewulf V, Bottjer SW (2005) Neurogenesis within the juvenile zebra finch telencephalic ventricular zone: a map of proliferative activity. *J Comp Neurol* **481**, 70–83.

Diao L, Sun W, Deng Q, et al. (2004) Development of the mouse retina: emerging morphological diversity of the ganglion cells. *J Neurobiol* **61**, 236–249.

Drenhaus U, Voigt T, Rager G (2007) Onset of synaptogenesis in the plexiform layers of the chick retina: a transmission electron microscopic study. *Microsc Res Tech* **70**, 329–335.

Edqvist PH, Hallböök F (2004) Newborn horizontal cells migrate bi-directionally across the neuroepithelium during retinal development. *Development* **131**, 1343–1351.

Evans BI, Browman HI (2004) Variation in the development of the fish retina. *American Fisheries Society Symposium* **40**, 145–166.

Ferreiro-Galve S, Rodríguez-Moldes I, Anadón R, et al. (2010) Patterns of cell proliferation and rod photoreceptor differentiation in shark retinas. *J Chem Neuroanat* **39**, 1–14.

Fischer AJ, Reh TA (2000) Identification of a proliferating marginal zone of retinal progenitors in postnatal chickens. *Dev Biol* **220**, 197–210.

Fischer AJ, Reh TA (2001) Müller glia are a potential source of neural regeneration in the postnatal chicken retina. *Nat Neurosci* **4**, 247–252.

Fischer AJ, Zelinka C, Gallina D, et al. (2014) Reactive microglia and macrophage facilitate the formation of Müller glia-derived retinal progenitors. *Glia* **62**, 1608–1628.

Francisco-Morcillo J, Sánchez-Calderón H, Kawakami Y, et al. (2005) Expression of Fgf19 in the developing chick eye. *Brain Res Dev Brain Res* **156**, 104–109.

Francisco-Morcillo J, Hidalgo-Sánchez M, Martín-Partido G (2006) Spatial and temporal patterns of proliferation and differentiation in the developing turtle eye. *Brain Res* **1103**, 32–48.

Gallina D, Todd L, Fischer AJ (2014) A comparative analysis of Müller glia-mediated regeneration in the vertebrate retina. *Exp Eye Res* **123**, 121–130.

Godinho L, Williams PR, Claassen Y, et al. (2007) Non-apical symmetric divisions underlie horizontal cell layer formation in the developing retina in vivo. *Neuron* **56**, 597–603.

Guduric-Fuchs J, Ringland LJ, Gu P, et al. (2009) Immunohistochemical study of pig retinal development. *Mol Vis* **15**, 1915–1928.

Hamburger V, Hamilton HL (1951) A series of normal stages in the development of the chick embryo. *J Morphol* **88**, 49–92.

Harahush BK, Hart NS, Green K, et al. (2009) Retinal neurogenesis and ontogenetic changes in the visual system of the brown banded bamboo shark, *Chiloscyllium punctatum* (Hemiscylliidae, Elasmobranchii). *J Comp Neurol* **513**, 83–97.

Hendrickson A, Yan YH, Erickson A, et al. (2007) Expression patterns of calretinin, calbindin and parvalbumin and their colocalization in neurons during development of Macaca monkey retina. *Exp Eye Res* **85**, 587–601.

Kitambi SS, Malicki JJ (2008) Spatiotemporal features of neurogenesis in the retina of medaka, *Oryzias latipes*. *Dev Dyn* **237**, 3870–3881.

Köppl C, Futterer E, Nieder B, et al. (2005) Embryonic and posthatching development of the barn owl (*Tyto alba*): reference data for age determination. *Dev Dyn* **233**, 1248–1260.

Kubota R, Hokoc JN, Moshiri A, et al. (2002) A comparative study of neurogenesis in the retinal ciliary marginal zone of homeothermic vertebrates. *Brain Res Dev Brain Res* **134**, 31–41.

Loeliger M, Rees S (2005) Immunocytochemical development of the guinea pig retina. *Exp Eye Res* **80**, 9–21.

Marín-Teva JL, Calvente R, Cuadros MA, et al. (1999a) Circumferential migration of ameboid microglia in the margin of the developing quail retina. *Glia* **27**, 226–238.

Marín-Teva JL, Cuadros MA, Calvente R, et al. (1999b) Naturally occurring cell death and migration of microglial precursors in the quail retina during normal development. *J Comp Neurol* **412**, 255–275.

Marín-Teva JL, Almendros A, Calvente R, et al. (1999c) Proliferation of actively migrating ameboid microglia in the developing quail retina. *Anat Embryol (Berl)* **200**, 289–300.

Murray JR, Varian-Ramos CW, Welch ZS, et al. (2013) Embryological staging of the Zebra Finch, *Taeniopygia guttata*. *J Morphol* **274**, 1090–1110.

Nag TC, Wadhwa S (2007) Morphological and neurochemical development of the human neural retina. *Neuroembryol Aging* **4**, 19–30.

Nice MM (1962) Development of behavior in precocial birds. pp 1–211. New York:Transactions Linnean Society of New York.

Okada M, Erickson A, Hendrickson A (1994) Light and electron microscopic analysis of synaptic development in Macaca monkey retina as detected by immunocytochemical labeling for the synaptic vesicle protein, SV2. *J Comp Neurol* **339**, 535–558.

Olea GB, Sandoval MT (2012) Embryonic development of *Columba livia* (Aves: Columbiformes) from an altricial-precocial perspective. *Rev Colomb Cienc Pecu* **25**, 3–13.

Olea GB, Hernando AB, Lombardo DM (2016) Heterochronic events in the ontogeny of *Columba livia*, *Coturnix coturnix*, and *Gallus gallus domesticus*. *Rev Colomb Cienc Pecu* **29**, 274–282.

Pavón-Muñoz T, Bejarano-Escobar R, Blasco M, et al. (2016) Retinal development in the gilthead seabream *Sparus aurata*. *J Fish Biol* **88**, 492–507.

Prada C, Puga J, Pérez-Méndez L, et al. (1991) Spatial and temporal patterns of neurogenesis in the chick retina. *Eur J Neurosci* **3**, 1187.

Rapaport DH, Robinson SR, Stone J (1985) Cytogenesis in the developing retina of the cat. *Aust N Z J Ophthalmol* **13**, 113–124.

Rapaport DH, Wong LL, Wood ED, et al. (2004) Timing and topography of cell genesis in the rat retina. *J Comp Neurol* **474**, 304–324.

Reese BE, Johnson PT, Baker GE (1996) Maturational gradients in the retina of the ferret. *J Comp Neurol* **375**, 252–273.

Robinson SR, Rapaport DH, Stone J (1985) Cell division in the developing cat retina occurs in two zones. *Brain Res* **351**, 101–109.

Rojas LM, Mitchell MA, Ramírez YM, et al. (2007) Comparative analysis of retina structure and photopic electroretinograms in developing altricial pigeons (*Columba livia*) and precocial Japanese quails (*Coturnix japonica japonica*). *Ornitol Neotrop* **18**, 503–518.

Sharma RK, Ehinger B (1997) Mitosis in developing rabbit retina: an immunohistochemical study. *Exp Eye Res* **64**, 97–106.

Sharma RK, O'Leary TE, Fields CM, et al. (2003) Development of the outer retina in the mouse. *Brain Res Dev Brain Res* **145**, 93–105.

Shirazi Fard S, All-Ericsson C, Hallböök F (2014) The heterogenic final cell cycle of chicken retinal Lim1 horizontal cells is not regulated by the DNA damage response pathway. *Cell Cycle* **13**, 408–417.

Smirnov EB, Puchkov VF (2004) Characteristics of cellular proliferation in the developing human retina. *Neurosci Behav Physiol* **34**, 643–648.

Snow RL, Robson JA (1994) Ganglion cell neurogenesis, migration and early differentiation in the chick retina. *Neuroscience* **58**, 399–409.

Snow RL, Robson JA (1995) Migration and differentiation of neurons in the retina and optic tectum of the chick. *Exp Neurol* **134**, 13–24.

Stark JM, Ricklefs RE (1998) *Avian Growth and Development*. New York: Oxford University Press. pp. 3–30.

Stone J, Egan M, Rapaport DH (1985) The site of commencement of retinal maturation in the rabbit. *Vision Res* **25**, 309–317.

Striedter GF, Charvet CJ (2008) Developmental origins of species differences in telencephalon and tectum size: morphometric comparisons between a parakeet (*Melopsittacus undulatus*) and a quail (*Colinus virgianus*). *J Comp Neurol* **507**, 1663–1675.

Villar-Cheda B, Abalo XM, Villar-Cervino V, et al. (2008) Late proliferation and photoreceptor differentiation in the transforming lamprey retina. *Brain Res* **1201**, 60–67.

Weber IP, Ramos AP, Strzyz PJ, et al. (2014) Mitotic position and morphology of committed precursor cells in the zebrafish retina adapt to architectural changes upon tissue maturation. *Cell Rep* **7**, 386–397.

Weidman TA, Kuwabara T (1968) Postnatal development of the rat retina. An electron microscopic study. *Arch Ophthalmol* **79**, 470–484.

Young RW (1985a) Cell proliferation during postnatal development of the retina in the mouse. *Brain Res* **353**, 229–239.

Young RW (1985b) Cell differentiation in the retina of the mouse. *Anat Rec* **212**, 199–205.